RSC Advances

PAPER

View Article Online
View Journal | View Issue

Open Access Article. Published on 14 November 2018. Downloaded on 10/23/2025 10:01:20 PM.
This article is licensed under a Creative Commons Attribution-NonCommercial 3.0 Unported Licence.

Check for updates

Cite this: *RSC Adv.*, 2018, **8**, 38384

Kinetic investigation for the catalytic reduction of nitrophenol using ionic liquid stabilized gold nanoparticles†

Sachin R. Thawarkar,*[a] Balu Thombare,[b] Bhaskar S. Munde[c] and Nageshwar D. Khupse *[d]

We demonstrate the synthesis of gold nanoparticles (AuNP) stabilized by 1-butyl-3-hexadecyl imidazolium bromide (Au@[C_4C_{16}Im]Br) and their use as a catalyst for the reduction of nitrophenol. The AuNPs show excellent stability in presence of [C_4C_{16}Im]Br ionic liquids for the reduction of 4-nitrophenol and 2-nitrophenol using $NaBH_4$ as a reducing agent. The detailed kinetics for the reduction of 4-nitrophenol and 2-nitrophenol were investigated and the catalytic activity of Au@[C_4C_{16}Im]Br was evaluated. The pseudo first-order rate constant (k_{app}) values for 4-nitrophenol was observed to be greater than that of 2-nitrophenol and explained on the basis of hydrogen bonding present in 2-nitrophenol. Au@[C_4C_{16}Im]Br showed good separability and reusability and hence, it can be used for the complete reduction of nitrophenols in multiple cycles. The Langmuir–Hinshelwood reaction mechanism is elucidated for reduction of 4-nitrophenol by Au@[C_4C_{16}Im]Br nanocatalyst on the basis of the k_{app} values. The thermodynamic activation parameters such as activation energy, enthalpy of activation and entropy of activation were determined and explained using the temperature dependent kinetics for the reduction of nitrophenol using Au@[C_4C_{16}Im]Br. The above results reveal that the Au@[C_4C_{16}Im]Br nanocatalyst demonstrates excellent catalytic performance for the reduction of nitrophenol by $NaBH_4$ at room temperature.

Received 5th September 2018
Accepted 29th October 2018

DOI: 10.1039/c8ra07404f

rsc.li/rsc-advances

1. Introduction

Metal nanoparticles of different sizes, shapes, and composition have many important catalytic applications[1–4] as well as applications in biosensing,[5] optoelectronics,[6] petroleum industries, chemical conversion, biology,[7] *etc.* Gold nanoparticles (AuNPs) have attracted considerable interest due to their exceptionally high surface-to-volume ratios and abundance of edge and corner atoms.[8,9] Recently, gold nanoparticles have attracted enormous attention in the field of chemical processes due to their unique stability, selectivity, and catalytic activities for transformation reactions.[10] The high surface energy of metal NPs makes the surface atoms very active, which leads fast aggregation of the metal NPs.[11] It is essential to use a capping agent to prevent the aggregation of AuNPs.[12,13] To synthesize stable metal NPs in solution, the addition of a stabilizing agent is required to prevent aggregation. Thiols have been most commonly used as a stabilizer for AuNPs. However, thiol-stabilized AuNPs are relatively inert. Hence, further replacement of thiols with other ligands may not be easy, thus affecting the labile nature of the AuNPs. Thus, surface bound ligands are used to maintain the nanostructures, but they can block the reactive surface sites, resulting in the reduction of catalytic activity. Therefore, to prepare stable colloidal NPs with sufficient lability, there needs to be a suitable selection of the surface ligand. Furthermore, the effect of capping agents on the catalytic activity of the NPs has been investigated and reported.[14] An inverse relationship between stability and catalytic activity has been observed. Hence, it is necessary to maintain stability and catalytic activity of the NPs by selecting suitable stabilizing ligands. Ionic liquids are also used as suitable capping agents for the AuNPs.[15,16] AuNPs stabilized with ionic liquids were synthesized and were observed to show excellent stability.[17] The interaction of the NPs with ionic liquids is occurs through the imidazolium ring, while the alkyl chain remains away from NP surface.[17]

The reduction of 4-nitrophenol is a very simple reaction for the analysis of reaction kinetics and improvement of catalytic activity.[18–21] Moreover, this reaction is a well-known model reaction for determining the activity of a catalyst because of the convenience of analyzing the progress of the reaction and the

[a]*Physical and Materials Chemistry Division, CSIR-National Chemical Laboratory, Dr. Homi Bhabha Road, Pune-411008, India. E-mail: sachinthawarkar@gmail.com*

[b]*Department of Physics, Savitribai Phule Pune University, Ganeshkhind, Pune 411007, India*

[c]*Department of Physics, K. K. M. College, Manwath, Parbhani 431505, India*

[d]*Centre for Materials for Electronics Technology (C-MET), Ministry of Electronics and Information Technology (Meit), Government of India, Panchawati, Off Pashan Road, Pune-411008, India. E-mail: nageshkhupse@gmail.com*

† Electronic supplementary information (ESI) available. See DOI: 10.1039/c8ra07404f

 This journal is © The Royal Society of Chemistry 2018

Open Access Article. Published on 14 November 2018. Downloaded on 10/23/2025 10:01:20 PM.
This article is licensed under a Creative Commons Attribution-NonCommercial 3.0 Unported Licence.

absence of by-products.[22] In general, nitrophenols are not reduced by $NaBH_4$ in aqueous or non-aqueous solutions without a catalyst. The reduction of nitro compounds to the corresponding amines is an important industrial reaction. Amines are the starting compounds for several synthesis processes as intermediates such as azo, imines, and amides and furthermore, these compounds can be converted to other important intermediates that have many applications in agriculture, pharmaceuticals, dyes, polymers and many of them are biologically active.[23–25] However, the disadvantage of the reaction for nitro compound reduction is the use of high temperatures, long reaction times and most importantly the use of costly catalysts. Therefore, it is necessary to develop a method for the conversion of 4-nitrophenol to 4-aminophenol in aqueous solution under mild conditions by using an appropriate catalyst. An aqueous solution of 4-nitrophenolate ion shows a peak at $\lambda_{max} = 400$ nm. The disappearance of this peak to form a new peak at 300 nm corresponds to the formation of *p*-aminophenol. This reaction has been greatly studied by many groups using noble metal NPs, dendrimers and nanorods as catalysts.[26–28] Several researchers have reported the reduction of nitrophenol by using AuNPs. Herein, we analyzed the efficiency of Au@[C_4C_{16}Im]Br for the catalytic reduction of nitrophenol. It is reported that various nanostructured materials have been used as catalysts for the reduction of nitrophenols under mild reaction conditions. For example, Au_{25} clusters, gold–palladium nanoalloys, gold nanowires and Au@Fe_3O_4 yolk–shell nanostructures, have been used as effective catalysts for the reduction of 4-nitrophenol.[29–31] Many reports indicate that the NPs used for the reduction of 4-nitrophenol follow two mechanisms: (1) Langmuir–Hinshelwood (L–H) mechanism and (2) Eley–Rideal (E–R) mechanism.[32–35] Several research groups have analyzed the kinetics of the reduction reaction by varying the concentration of 4-nitrophenol and $NaBH_4$ for determining the reaction mechanism.[2,35,36] It has also been illustrated that the mechanism for the reduction reaction of 4-nitrophenol and $NaBH_4$ involves adsorption of 4-nitrophenol on the surface of the catalyst, and the reaction could proceed through the L–H mechanism. However, in the E–R mechanism, only one species is adsorbed on the surface of the catalyst, and the reaction is promoted.

In the present study, we synthesized ionic liquid [C_4C_{16}Im]Br-stabilized AuNPs for the catalytic reduction of 4-nitrophenol and 2-nitrophenol. We also studied the kinetics and catalytic activity of the reduction of nitrophenol using Au@[C_4C_{16}Im]Br. The L–H mechanism has been explained on the basis of kinetic data and catalytic activity of Au@[C_4C_{16}Im]Br for the reduction reaction of 4-nitrophenol. This study also proposes a deep insight into the kinetics of the reduction of nitrophenol from thermodynamic parameters such as activation energy (ΔE_a), enthalpy of activation ($\Delta H^{\#}$) and entropy of activation ($\Delta S^{\#}$).

2. Experimental section

2.1. Kinetic measurements

An aqueous solution of 1×10^{-4} M of 4-nitrophenol was prepared and then, 20 mg of Au@[C_4C_{16}Im]Br catalyst was added to this solution. Finally, an aqueous solution 1×10^{-3} M of $NaBH_4$ was added to above mixture. This reaction was performed in N_2 atmosphere. The reaction progress was monitored at 400 nm in UV, which is the λ_{max} of 4-nitrophenolate ion, by using a UV-vis adsorption spectrophotometer. The absorption peak at 400 nm decreases with time, indicating the reduction of 4-nitrophenol. The pseudo first-order rate constants (k_{app}) were calculated by fitting the first-order rate constant equation for $\ln(A_0/A_t)$ values against t (s) with a linear fit, where, A_0 and A_t are the initial absorbance and absorbance after a given time, respectively. The correlation coefficients, *i.e.*, r values for this linear fits, varied from 0.96 to 0.99. The k_{app} values were obtained with an accuracy of ±5%. The experimental k_{app} values are the average values for triplicate experiments. The effect of temperature on the k_{app} values were studied by varying the temperature from 283.15 to 318.15 K.

2.2. Transmission electron microscopy (TEM)

To determine the morphology and size of Au@[C_4C_{16}Im]Br present in the aqueous solution, one drop of solution was placed on a carbon-coated Cu grid and air dried. The image was taken by placing the sample-containing the grid in a TECHNAI G2 20 S-TWIN high-resolution transmission electron microscope operating with a LaB6 filament and at a voltage of 200 kV.

3. Results and discussion

We synthesized ionic liquid-stabilized AuNPs according to a procedure reported in literature.[17] For this, an aqueous solution of [C_4C_{16}Im]Br and a solution of $HAuCl_4$ were mixed in the molar ratio of 10 : 1. $NaBH_4$ is added to this mixture dropwise with constant stirring. The color of the solution turned red wine, confirming the formation of AuNPs, as shown in Fig. S1.† Centrifugation was performed immediately after the formation of Au@[C_4C_{16}Im]Br to remove impurities and also obtain the AuNPs with an appropriate size distribution. The size of Au@[C_4C_{16}Im]Br was observed to be about 10 nm, as shown in the TEM image (Fig. 1). The as-prepared solution of Au@[C_4C_{16}Im]Br remains stable for more than a month without agglomeration in the aqueous solution. We confirmed the formation of AuNPs capped with [C_4C_{16}Im]Br with the help of UV-vis spectroscopy. The

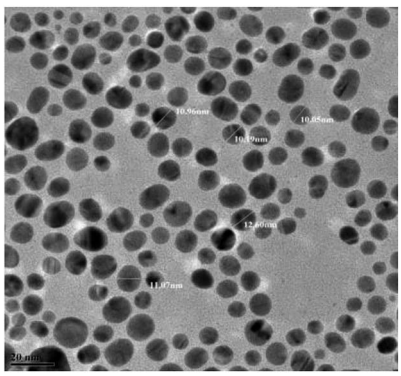

Fig. 1 TEM image of Au@[C_4C_{16}Im]Br nanoparticles in water.

Open Access Article. Published on 14 November 2018. Downloaded on 10/23/2025 10:01:20 PM.
This article is licensed under a Creative Commons Attribution-NonCommercial 3.0 Unported Licence.

stability of the AuNPs was due to the higher alkyl chain length of the ionic liquid, which was confirmed by ^{1}H-NMR and surface enhanced Raman spectroscopy.[37] Thus, Au@[C_4C_{16}Im]Br is stable due to protection of the imidazolium ring *via* the C-2 proton as well as steric hindrance due to the alkyl chains of the imidazolium ionic liquid. Moreover, a charged layer of ions from the ionic liquids was produced around the AuNPs, which repelled other AuNPs and enhanced the stability of Au@[C_4C_{16}Im]Br.

3.1. Catalytic reduction of 4-nitrophenol and 2-nitrophenol using Au@[C_4C_{16}Im]Br catalyst

The catalytic reduction of 4-nitrophenol and 2-nitrophenol to their corresponding derivatives, 4-aminophenol and 2-aminophenol in the presence of $NaBH_4$ was chosen as the model reaction to investigate the catalytic activity of Au@[C_4C_{16}Im]Br. Fig. 2 shows the time-dependent UV-vis absorption spectra for the reduction of 4-nitrophenol using the Au@[C_4C_{16}Im]Br catalyst. An aqueous solution of 4-nitrophenol shows an absorption peak at 318 nm in the UV visible region, but on addition of $NaBH_4$, the peak shifts to 400 nm due to the formation of 4-nitrophenolate ions. The peak intensity at 400 nm immediately starts to decrease with the formation of a new additional peak at 300 nm, which corresponds to the formation of 4-aminophenol. In addition, the yellow color solution of 4-nitrophenol begins to disappear with time and a colourless solution is observed, which indicates the completion of the reaction. We have also performed the reduction of 4-nitrophenol in the absence of Au@[C_4C_{16}Im]Br. The peak corresponding to the phenolate ion at 400 nm remained unaffected with time, suggesting that the reduction of 4-nitrophenol does not occur in the absence of a catalyst.

A similar experiment was performed for 2-nitrophenol and similar results as for 4-nitrophenol were observed. Nitrogen was purged before the addition of $NaBH_4$ to remove dissolved oxygen in water, which reacts at a faster rate with borohydride than nitrophenol.

3.2. Kinetic analysis of nitrophenols

The calculated rate constant of the reaction is a pseudo first-order rate constant (k_{app}) due to the presence of excess $NaBH_4$ compared with nitrophenols. The apparent rate constant was calculated using eqn (1) for a first-order reaction.[38]

$$\ln\left(\frac{A_t}{A_0}\right) = -k_{app}t \quad (1)$$

where A_t is the absorbance of nitro compounds at time in second (s), k_{app} is the apparent rate constant.

The reaction kinetics was investigated by measuring the k_{app} values for the reduction of nitrophenol. The rate of reaction was determined by measuring the decrease in the absorption intensity at $\lambda_{max} = 400$ nm of the phenolate ion with time for the reduction of nitrophenols. k_{app} was calculated from the slope obtained by plotting $\ln(A_t/A_0)$ *vs.* time. The k_{app} values were determined for 4-nitrophenol and 2-nitrophenol and given in Table 1.

According Table 1, the k_{app} value for 4-nitrophenol is 1.10×10^{-4} s^{-1}, which is higher than that for 2-nitrophenol (7.73×10^{-5} s^{-1}) using the Au@[C_4C_{16}Im]Br catalyst. The difference in k_{app} values is explained on the basis of the position of the hydroxyl substituent in the aromatic ring. In nitrophenols, lower k_{app} value for 2-nitrophenol than that of 4-nitrophenol is achieved by merely changing the position of the hydroxyl group from 4 to 2 position. The reduction occurs by the donation of an electron from $NaBH_4$ to $-NO_2$ group. The *para* mesomeric donation is more effective than *ortho* mesomeric donation. Thus, 2-nitrophenol is more stabilized due to the existence of intramolecular hydrogen bonding between the –OH and $-NO_2$ groups and therefore, 2-nitrophenol is less reactive for the reduction reaction compared to 4-nitrophenol.[38]

Furthermore, we determined the turnover number (TON) and the turn over frequency (TOF) of Au@[C_4C_{16}Im]Br catalyst to decide the efficiency of the catalyst. In a heterogeneous catalysis reaction, the TON of catalyst is the number of substrate molecules that can convert into products using 1 g of catalyst, while TOF is calculated as TON/time. The substrate and catalyst concentrations used for the reduction are 1.1×10^{-4} M and 0.02 g L^{-1}, respectively. The TOF was found to be 3.8×10^{-3} molecules per g per s for Au@[C_4C_{16}Im]Br catalyst using the following equation:

$$\mathrm{TOF} = \frac{m_i X x}{100\ \mathrm{wt}} \quad (2)$$

where m_i is the initial number of moles nitrophenol, X is the conversion of nitrophenol, x is the molecular weight of nitrophenol, w is the mass of catalyst used in the reaction (g), and t is the reaction time (h).

We also tested the catalytic activity after recycling the Au@[C_4C_{16}Im]Br catalyst, and it was observed to be easily recyclable and reusable. The Au@[C_4C_{16}Im]Br catalyst was recycled from

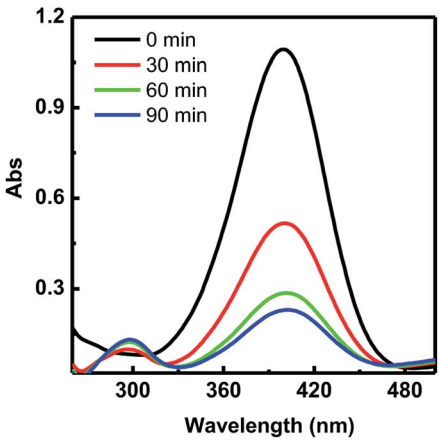

Fig. 2 Time-dependent UV-vis absorption spectra of 4-nitrophenol reduced by $NaBH_4$ in the presence of Au@[C_4C_{16}Im]Br catalyst.

Table 1 The k_{app} values for the reduction of nitrophenols in the presence of Au@[C_4C_{16}Im]Br as catalyst at 298.15 K

S. No.	Nitrophenols	k_{app} (s^{-1})
1	4-Nitrophenol	1.10×10^{-4}
2	2-Nitrophenol	7.73×10^{-5}

Open Access Article. Published on 14 November 2018. Downloaded on 10/23/2025 10:01:20 PM.
This article is licensed under a Creative Commons Attribution-NonCommercial 3.0 Unported Licence.

the reaction mixture by centrifugation. The catalytic activity of the recycled Au@[C_4C_{16}Im]Br catalyst was examined on the basis of k_{app} values for the reduction of 4-nitrophenol. The concentration of the catalyst was 20 ppm. After recycling, the k_{app} value was found to be 2.75×10^{-5} s^{-1}, which was noted to be lower than that of the pure catalyst. The lower k_{app} value for the Au@[C_4C_{16}Im]Br catalyst may be due to loss of a certain amount of catalyst after the first catalytic cycle by the centrifugation and washing processes. We recorded TEM images of Au@[C_4C_{16}Im]Br after the first cycle, as shown in Fig. 3. The shape and size of AuNPs are not affected, which indicates that the AuNPs are stable enough to demonstrate catalytic activity. Thus, the decrease in k_{app} value after the first use is due to the loss in amount of catalyst during recycling.

3.3. Reaction mechanism

The Langmuir–Hinshelwood (L–H) mechanism has been proposed by Wunder *et al.* for investigating kinetically controlled surface catalytic reduction reactions of 4-nitrophenol by Au/Pt nanostructures immobilized with spherical polyelectrolyte brushes.[35] According to this mechanism, the metallic nanostructure provides a surface for the catalytic reduction process to take place.[20,39] The BH_4^- ions adsorb on the surface of AuNPs and transfer hydrogen species to the surface of the AuNPs. At the same time, 4-nitrophenol also adsorbs on the surface and is reduced to 4-aminophenol by the BH_4^- ions. Finally, 4-aminophenol detaches to free the surface of the NPs for the next catalytic cycle to begin. The catalytic reduction of the nitrophenols with Au@[C_4C_{16}Im]Br is a heterogeneous catalytic reduction reaction. The heterogeneous catalytic reduction reaction can take place either by the L–H or the E–R (Eley–Rideal mechanism). In the case of the E–R mechanism, only one of the reactant molecules is adsorbed on the surface of the catalyst and reacts with the other reactant molecules. In the case of the L–H mechanism, both substrate molecules, nitrophenol and BH_4^-, get adsorbed on the surface of the catalyst and then, the reaction is occurs. A reaction mechanism for the reduction of 4-nitrophenol can be investigated in two ways: (1) determination of k_{app} values with different concentration of 4-nitrophenol and (2) determination of k_{app} values with different concentrations of $NaBH_4$. In the L–H mechanism, the k_{app} value decreases with the concentration of 4-nitrophenol, while it increases with the concentration of $NaBH_4$. However, in case of the E–R mechanism, the k_{app} value increases with the concentration of 4-nitrophenol. We know that the reduction of 4-nitrophenol is a first-order reaction with respect to 4-nitrophenol. The k_{app} values of the catalytic reduction reaction are proportional to the surface area of the materials. The kinetic rate constant can be determined as[40–42]

$$\frac{dc_{NP}}{dt} = kc_{NP} = k_1\, Sc_{NP} \tag{3}$$

In terms of the Langmuir–Freundlich isotherm

$$\theta_i = \frac{(k_i c_i)^{n_i}}{1 + \sum_{j=1}^{N}(K_j c_j)} \tag{4}$$

where θ_i is the surface coverage of substrate i, k_i the adsorption constant of the respective components, c_i the concentration and n the heterogeneity of the surface materials. The rearrangement of eqn (4) gives an eqn (5), which can be used to model the catalytic activity.

$$-\frac{dc_{NP}}{dt} = \frac{kS(K_{NP}c_{NP})^n(K_{BH_4}c_{BH_4})^m}{(1 + (K_{NP}c_{NP})^n + (K_{BH_4}c_{BH_4})^m)^2} = k_{app}c_{NP} \tag{5}$$

Thus, k_{app} is given by

$$\theta_i = \frac{kSK_{NP}{}^n c_{NP}{}^{n-1}(K_{BH_4}c_{BH_4})^m}{(1 + (K_{NP}c_{NP})^n + (K_{BH_4}c_{BH_4})^m)^2} \tag{6}$$

where k is the molar rate constant per square meter of catalyst, K_{NP} is the adsorption coefficient of the nitrocompounds, and K_{BH_4} is the adsorption coefficient of BH_4^-. The plot of the k_{app} values *versus* the concentration of 4-nitrophenol at a fixed concentration of $NaBH_4$ of 1×10^{-3} M in the presence of Au@[C_4C_{16}Im]Br at 298.15 K are given in Fig. 4. The k_{app} values

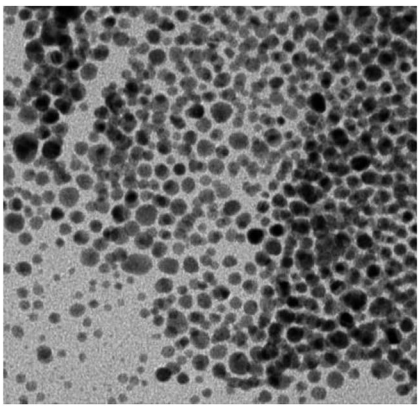

Fig. 3 TEM image of Au@[C_4C_{16}Im]Br after first recycle.

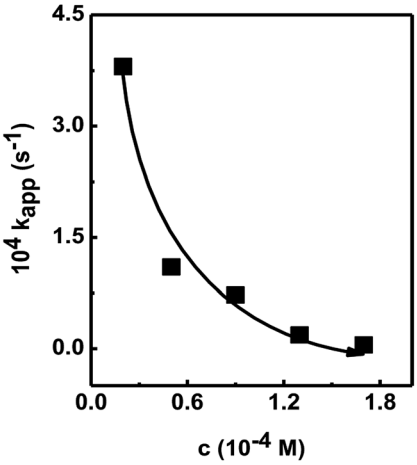

Fig. 4 Plot of k_{app} *vs.* conc. of 4-nitrophenol in the presence of Au@[C_4C_{16}Im]Br catalyst. Lines drawn to guide the reader's eye.

Open Access Article. Published on 14 November 2018. Downloaded on 10/23/2025 10:01:20 PM.
This article is licensed under a Creative Commons Attribution-NonCommercial 3.0 Unported Licence.

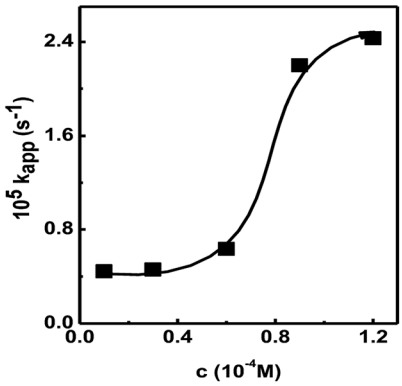

Fig. 5 Plot of k_{app} *vs.* conc. $NaBH_4$ in the presence of Au@[C_4C_{16}Im]Br catalyst. Lines drawn to guide the reader's eye.

Table 2 Temperature dependent k_{app} values for the reduction of 4-nitrophenol and 2-nitrophenol

S. No.	Temperature (K)	4-Nitrophenol, k_{app} (s^{-1}) (10^{-4})	2-Nitrophenol, k_{app} (s^{-1}) (10^{-4})
1	293.15	1.03	0.25
2	298.15	1.10	0.77
3	303.15	2.14	1.74
4	310.15	9.84	5.14
5	318.15	17.8	6.04

decreased with increase in concentration of 4-nitrophenol. Similarly, the plot of k_{app} values *versus* the concentration of $NaBH_4$ with a fixed concentration of 4-nitrophenol of 1.1×10^{-4} M in the presence of Au@[C_4C_{16}Im]Br at 298.15 K is given in Fig. 5. The k_{app} values increased with increase in the concentration of $NaBH_4$. Thus, the nonlinear variation of the k_{app} values with respect to the concentration of 4-nitrophenol and $NaBH_4$ shows that the reduction of 4-nitrophenol follows the L–H mechanism. The number of molecules adsorbed at the surface of the Au@[C_4C_{16}Im]Br nanocatalyst increases with the increase in the concentration of 4-nitrophenol and hence, the surface becomes saturated by 4-nitrophenol molecules.

This leads to a decrease in concentration of BH_4^- ions approaching the surface of the Au@[C_4C_{16}Im]Br catalyst, hence lowering the rate of hydrogen transfer from BH_4^- ion to the 4-nitrophenol molecule. This confirms that the Au@[C_4C_{16}Im]Br catalyzed reduction of nitrophenol occurs according to the L–H mechanism.

3.4. Thermodynamics study of kinetics of the reduction of nitrophenol

We investigated the temperature-dependent reduction reaction of 4-nitrophenol and 2-nitrophenol catalyzed by Au@[C_4C_{16}Im]Br at five different temperatures. The k_{app} values for the reduction of 4-nitrophenol and 2-nitrophenol increased with the increase in temperature, as given in Table 2, because of an increase in the diffusion of reactant molecules.

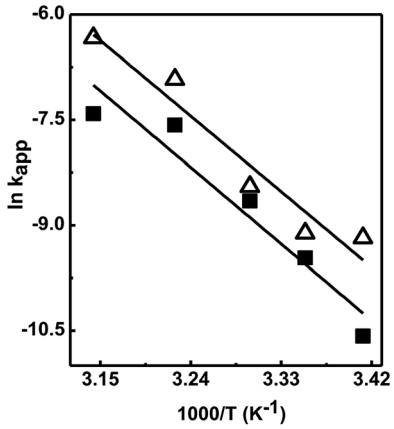

Fig. 6 The Arrhenius plots of ln k_{app} *vs.* 1/*T* for the reduction reaction of 4-nitrophenol (Δ) and 2-nitrophenol (■) with $NaBH_4$ at different temperature.

The activation energies (E_a) for the reduction reaction of 4-nitrophenol and 2-nitrophenol were determined from the Arrhenius eqn (7):[43–45]

$$\ln k = \ln A - \frac{E_a}{RT} \tag{7}$$

where E_a, is activation energy, A is Arrhenius factor, T is temperature and R is the ideal gas constant. The values of E_a were determined from the slope of the plot of ln k *vs.* 1/T, as shown in Fig. 6 and Table 3.

The activation parameters for the catalytic reduction of nitrophenol using AuNPs are summarized in Table 3. The E_a values for the reduction of nitrocompounds, mainly for 4-nitrophenol catalyzed by different metals and metal NPs, have been determined by many research groups. For example, the E_a values for the reduction of 4-nitrophenol using dendrimer-encapsulated palladium NPs and for a palladium nanocage structure are 30 kJ mol^{-1} and 109 kJ mol^{-1}, respectively.[24]

In this study, the activation energies E_a for 4-nitrophenol and 2-nitrophenol are 99.40 and 100.59 kJ mol^{-1}, respectively which are in good agreement with literature values and confirms that the reaction follows the L–H mechanism.

Thermodynamic parameters such as activation enthalpy ($\Delta H^{\#}$) and activation entropy ($\Delta S^{\#}$) for the reduction of 4-nitrophenol and 2-nitrophenol were determined using the Eyring equation (eqn (8)).[38]

$$\ln \frac{k_{app}}{T} = \ln\left(\frac{k_B}{h}\right) + \frac{\Delta S^{\#}}{R} - \frac{\Delta H^{\#}}{RT} \tag{8}$$

$$\Delta G = \Delta H - T\Delta S \tag{9}$$

where k_{app} is the rate constant (s^{-1}), R is the universal gas constant, T is temperature (K), h is the Plank constant, k_B is the Boltzmann constant, and ΔG is the Gibb's free energy. The thermodynamic parameters $\Delta H^{\#}$ and $\Delta S^{\#}$ were obtained from Fig. S2† and represented in Table 3.

The values of k_{app} were 1.10 and 0.77 s^{-1}, corresponding to 4-nitrophenol and 2-nitrophenol, respectively. Moreover, the E_a

Open Access Article. Published on 14 November 2018. Downloaded on 10/23/2025 10:01:20 PM.
This article is licensed under a Creative Commons Attribution-NonCommercial 3.0 Unported Licence.

Table 3 Thermodynamic parameters $\Delta H^{\#}$, $\Delta S^{\#}$, $\Delta G^{\#}$ and E_a for the reduction of nitrophenols using Au@[C_4C_{16}Im]Br as catalyst

	Activation parameters			
Nitrophenols	E_a (kJ mol^{-1})	$\Delta H^{\#}$ (kJ mol^{-1})	$\Delta S^{\#}$ (kJ mol^{-1} K^{-1})	$\Delta G^{\#}$ (kJ mol^{-1})
4-Nitrophenol	99.40	96.85	143.33	54.12
2-Nitrophenol	100.59	98.06	141.17	55.81

value is higher for 2-nitrophenol compared with that of 4-nitrophenol, which reflects the rate constant (k_{app}) data. Similar trend is observed for other activation parameters $\Delta H^{\#}$ and $\Delta S^{\#}$. To proceed with the reduction reaction, for 2-nitrophenol to adsorbs on the catalyst surface, it needs to cross a higher energy barrier compared with that for 4-nitrophenol. Thus, the reactivity of nitrophenol is dependent on the substitution position of the hydroxyl group, which forms the intramolecular hydrogen bond with the nitro group; this is also confirmed from the kinetic data. The insignificant difference in reactivity of the nitrophenols is observed due to the different ability of the nitrophenols to form intramolecular hydrogen bonds. Hence, the AuNPs in the presence of [C_4C_{16}Im]Br show excellent catalytic activity. The detailed mechanism has been explained in the earlier section.

4. Conclusions

In conclusion, we synthesized and characterized ionic liquid-stabilized Au@[C_4C_{16}Im]Br in water with an average size of 10 nm. The catalytic activity of Au@[C_4C_{16}Im]Br for the reduction of nitrophenols in the presence of $NaBH_4$ was examined. (1) The kinetics of reduction of nitrophenols was investigated using Au@[C_4C_{16}Im]Br as a catalyst, and excellent catalytic activity with good recyclability was observed over multiple cycles of reduction of nitrophenols. (2) The k_{app} values for the reduction of 4-nitrophenol is higher than that for the reduction of 2-nitrophenol because of the intramolecular hydrogen bonding present in 2-nitrophenol. (3) The L–H reaction mechanism for the reduction of nitrophenols by Au@[C_4C_{16}Im]Br was confirmed on the basis of the k_{app} values and thermodynamic parameters. (4) Thermodynamic parameters such as $\Delta H^{\#}$, $\Delta S^{\#}$, $\Delta G^{\#}$ and E_a for the reduction of nitrophenol were determined by temperature-dependent kinetic studies using the Arrhenius and Eyring equations. The results obtained in this investigation are useful for the fabrication of highly efficient metal nanocatalysts using ionic liquids as stabilizing agents for the reduction of nitrophenols.

Conflicts of interest

There are no conflicts to declare.

Acknowledgements

NDK acknowledges SERB, New Delhi for Young Scientist Research Grant (YSS/2015/001229). The authors appreciate the anonymous reviewers for offering constructive evaluation of the study. S. R. T. thanks CSIR, New Delhi, for awarding him a Senior Research Fellowship and Dr Anil Kumar NCL Pune thanked for Scientific and Constructive suggestions and experimental facility.

References

1 B. Hinnemann, P. G. Moses, J. Bonde, K. P. Jørgensen, J. H. Nielsen, S. Horch, I. Chorkendorff and J. K. Nørskov, *J. Am. Chem. Soc.*, 2005, **127**, 5308–5309.
2 M. Kohantorabi and M. R. Gholami, *Ind. Eng. Chem. Res.*, 2017, **56**, 1159–1167.
3 Z. Wang, R. Su, D. Wang, J. Shi, J. Wang, Y. Pu and J. F. Chen, *Ind. Eng. Chem. Res.*, 2017, **56**, 13610–13617.
4 M. H. Rashid and T. K. Mandal, *J. Phys. Chem. C*, 2007, **111**, 16750–16760.
5 A. Virel, L. Saa and V. Pavlov, *Anal. Chem.*, 2009, **81**, 268–272.
6 M. Breton, G. Prével, J. F. Audibert, R. Pansu, P. Tauc, B. Le Pioufle, O. Français, J. Fresnais, J. F. Berret and E. Ishow, *Phys. Chem. Chem. Phys.*, 2011, **13**, 13268–13276.
7 J. Li, Z. Shen, X. Ma, W. Ren, L. Xiang, A. Gong, T. Xia, J. Guo and A. Wu, *ACS Appl. Mater. Interfaces*, 2015, **7**, 5574–5582.
8 S. M. Ansar and C. L. Kitchens, *ACS Catal.*, 2016, **6**, 5553–5560.
9 M. H. Rashid, R. R. Bhattacharjee, A. Kotal and T. K. Mandal, *Langmuir*, 2006, **22**, 7141–7143.
10 X. Bai, Y. Gao, H. Liu and L. Zheng, *J. Phys. Chem. C*, 2009, **113**, 17730–17736.
11 B. P. Binks, A. Desforges and D. G. Duff, *Langmuir*, 2007, **23**, 1098–1106.
12 J. Huang and Y. Wang, *J. Phys. Chem. B*, 2007, **111**, 7735–7741.
13 C. M. Phan and H. M. Nguyen, *J. Phys. Chem. A*, 2017, **121**, 3213–3219.
14 X. Bai, H. Ma, X. Li, B. Dong and L. Zheng, *Langmuir*, 2010, **26**, 14970–14974.
15 J. T. Lu, J. C. Lin, M. C. Lin, N. D. Khupse and I. J. B. Lin, *Langmuir*, 2014, **30**, 10440–10448.
16 P. Wasserscheid and T. Welton, *Ionic liquids in synthesis*, Wiley-VCH Verlag GmbH and Co. GaA, 2008.
17 S. Thawarkar, B. Thombare and N. D. Khupse, *New J. Chem.*, 2017, **41**, 12989–12995.
18 Y. Yang, Y. Ren, C. Sun and S. Hao, *Green Chem.*, 2014, **16**, 2273.
19 S. A. Lawrence, *Amines: Synthesis, Properties and Applications*, Cambridge University Press, New York, 2004.
20 Y. Zhang, Z. Cui, L. Li, L. Guo and S. Yang, *Phys. Chem. Chem. Phys.*, 2015, **17**, 14656–14661.

Open Access Article. Published on 14 November 2018. Downloaded on 10/23/2025 10:01:20 PM.
This article is licensed under a Creative Commons Attribution-NonCommercial 3.0 Unported Licence.

21 (*a*) P. Deka, R. C. Deka and P. Bharali, *New J. Chem.*, 2014, **38**, 1789; (*b*) H. Yang, S. Li, X. Zhang, X. Wang and J. Ma, *J. Mater. Chem. A*, 2014, **2**, 12060–12067.
22 T. Aditya, A. Pal and T. Pal, *Chem. Commun.*, 2015, **51**, 9410–9431.
23 k. Layek, M. L. Kantam, M. Shirai, D. Nishio-Hamane, T. Sasaki and H. Maheswaran, *Green Chem.*, 2012, **14**, 3164.
24 M. A. Mahmoud, F. Saira and M. A. El-Sayed, *Nano Lett.*, 2010, **10**, 3764–3769.
25 C. Y. Wang, C. F. Fu, Y. H. Liu, S. M. Peng and S. T. Liu, *Inorg. Chem.*, 2007, **46**, 5779–5786.
26 Z. D. Pozun, S. E. Rodenbusch, E. Keller, K. Tran, W. Tang, K. J. Stevenson and G. J. Henkelman, *J. Phys. Chem. C*, 2013, **117**, 7598–7604.
27 B. Baruah, G. J. Gabriel, M. J. Akbashev and M. E. Booher, *Langmuir*, 2013, **29**, 4225–4234.
28 N. Pradhan, A. Pal and T. Pal, *Langmuir*, 2001, **17**, 1800–1802.
29 N. Bingwa, R. Patala, J. H. Noh, M. J. Ndolomingo, S. Tetyana, S. Bewana and R. Meijboom, *Langmuir*, 2017, **33**, 7086–7095.
30 F. Lin and R. Doong, *J. Phys. Chem. C*, 2017, **121**, 7844–7853.
31 A. Shivhare, S. J. Ambrose, H. Zhang, R. W. Purves and R. W. Scott, *Chem. Commun.*, 2013, **49**, 276–278.
32 Y. Khalavka, J. Becker and C. Sönnichsen, *J. Am. Chem. Soc.*, 2009, **131**, 1871–1875.
33 H. Zhang, X. Li and G. Chen, *J. Mater. Chem.*, 2009, **19**, 8223.
34 M. Hajfathalian, K. D. Gilroy, A. Yaghoubzade, A. Sundar, T. Tan, R. A. Hughes and S. Neretina, *J. Phys. Chem. C*, 2015, **119**, 17308–17315.
35 S. Wunder, F. Polzer, Y. Lu, Y. Mei and M. J. Ballauff, *J. Phys. Chem. C*, 2010, **114**, 8814–8820.
36 S. Gu, S. Wunder, Y. Lu, M. Ballauff, R. Fenger, K. Rademann, B. Jaquet and A. Zaccone, *J. Phys. Chem. C*, 2014, **118**, 18618–18625.
37 H. S. Schrekker, M. A. Gelesky, M. P. Stracke, C. M. L. Schrekker, G. Machado, S. R. Teixeira, J. C. Rubim and J. Dupont, *J. Colloid Interface Sci.*, 2007, **316**, 189–195.
38 S. R. Thawarkar, N. D. Khupse and A. Kumar, *ChemistrySelect*, 2017, **2**, 6833–6843.
39 N. C. Antonels and R. Meijboom, *Langmuir*, 2013, **29**, 13433–13442.
40 M. Li and G. Chen, *Nanoscale*, 2013, **5**, 11919.
41 L. Glasser, *J. Chem. Educ.*, 1979, **56**, 22.
42 N. Bingwa and R. Meijboom, *J. Phys. Chem. C*, 2014, **118**, 19849–19858.
43 S. Saha, A. Pal, S. Kundu, S. Basu and T. Pal, *Langmuir*, 2010, **26**, 2885–2893.
44 J. Tang, Z. Shi, R. M. Berry and K. C. Tam, *Ind. Eng. Chem. Res.*, 2015, **54**, 3299–3308.
45 T. Zhou, T. Liu, Z. Zhang, G. Zhang, F. Wang, X. Wang, S. Liu, H. Zhang, S. Wang and J. Ma, *J. Solid State Chem.*, 2018, 11–17.

 This journal is © The Royal Society of Chemistry 2018